International Research Journal of Engineering and Technology (IRJET) e-ISSN: 2395-0056
Volume: 04 Special Issue: 09 | Sep -2017 www.irjet.net p-ISSN: 2395-0072

One Day International Seminar on Materials Science & Technology (ISMST 2017)
4th August 2017
Organized by
Department of Physics, Mother Teresa Women's University, Kodaikanal, Tamilnadu, India

Nano Tailoring of MnO2 doped Multiwalled carbon nanotubes as electrode materials for supercapacitor

R.Ramesh kannan[1,*] S.Karthick Kumar[2]and M.Sivabharathy[2]

[1]Research and Development Centre, Bharathiyar University, Coimbatore, Tamil nadu, India
[2]Department of Physics, Sethu Institute of Technology, Virudunagar, Tamil nadu, India

---

Abstract - *Manganese decorated Multiwalled carbon nanotubes(MCNT) were synthesized through a simple solvo thermal method. The surface morphology and structural analyses of the MnO_2 doped MCNT were done using Transmission electron microscope (TEM), Field emission scanning electron microscopy (FESEM) and X-ray diffraction (XRD) methods. The compositions of the prepared samples were obtained using Energy dispersive spectroscopy (EDS). Morphological studies revealed that a three-dimensional hierarchy architecture built with a highly porous film of interconnected MnO_2 found on MCNT surface. The XRD and EDS results revealed that the prepared samples are in pure form without any impurities. It also reveals that birnessite-type MnO_2 is formed through the solvo thermal synthesis. The Optical properties of the prepared samples were examined by UV-visible spectrometer. The IR studies were carried out using Fourier transform infrared spectroscopy (FTIR) and Raman Spectroscopy.*

Key Words: MCNT, MnO_2, MnO_2 doped MCNT, Optical studies, Supercapacitor

1. INTRODUCTION

Energy storing devices are an important for the development of alternative energy sources [1]. Super capacitor is one of the promising energy storage devices due to its high specific capacitance, good cyclical stability and fast charge-discharge process, compare to rechargeable batteries [2-4]. The electrode material of the super capacitor is the key component to determine the performance of the super capacitor. Carbon based electrode material; metal oxide electrode material and conductive polymer electrode material are commonly employed electrode material in super capacitors [5-6]. Carbon based electrode material show stable cycle performance and high coulomb efficiency, but exhibits low specific capacitance. The conducting polymer and transition metal oxide electrode have high specific capacitance, low cycling stability [6].

Manganese oxide is well known for the manufacture of batteries, glasses, ceramics and find application in zinc smelting industry. Current research work focuses on manganese oxides because of their distinctive physical, chemical properties and finds applications in catalysis, ion exchange, molecular adsorption, biosensor, and energy storage [7]. In particular, manganese dioxide [MnO_2] has been considered as a promising electrode material for super capacitors because of its low cost and its eco friendly nature, excellent capacitive performance in aqueous electrolytes [8]. The charge storage in aqueous electrolytes is based on the adsorption of cations at the surface of the electrode material. In order to attain high capacitive performance, a large surface area and a fast ion/electron transport of the electrode material are essential [9-10]. Hence the research work concentrates on the synthesis of nanostructure MnO_2 as the nano scale powder, which provides not only a high specific surface area, but also a fast ion and electron transport. Various forms of MnO_2 including nanorods [11], nanotubes, nanosheets, nanoflakes [12], nanospheres [13] and nanoflowers [14] have been reported in the literature. However, specific capacitance value obtained for various nanostructure of MnO_2 electrodes were found to be lower than the theoretical value. So capacitive performance of MnO_2 is improved by adding additives. Carbon nanotubes have small density, large surface area because they exhibited good electrical and thermal conductivity are used as an ideal electrode material to form a large electrical double layer capacitor. CNT can also be act as the carrier material which increases the specific capacitance and electric conductivity of the material coated on it [15-16]. From literature it is understood the MnO_2 incorporation improves the capacitance of the CNT assembly, the overall specific capacitance is less than 200 F/g. Hence depositing a highly porous MnO_2 layer on the CNTs would help to achieve this goal. However, a facile and fast synthesis of a uniformly distributed MnO_2 porous layer on the CNTs is still a challenge. It could be a beneficial design if one of the nanostructures [nanowire, nanorod, nanoflake, etc.] of MnO_2 could be transferred onto the CNTs as this hierarchy architecture may be able to provide a large specific surface area [due to the porous feature of the MnO_2 sheath] and a fast electron and ion transport [due to the support of the CNT core and the formation of the nano scopic MnO_2 phase] [17-18].

One Day International Seminar on Materials Science & Technology (ISMST 2017)
4th August 2017
Organized by
Department of Physics, Mother Teresa Women's University, Kodaikanal, Tamilnadu, India

2. EXPERIMENTAL

A Commercial sample of multiwalled carbon nanotubes of dimensions (Outer diameter: 10±1nm, Inner diameter: 4.5±0.5 nm & Length: 3-6µm, surface area 280-350 m^2/g (BET), obtained from south west nano technologies.Inc. USA). This commercial sample was produced by the Catalytic chemical vapor deposition (CCVD) method and its purity is greater than 98%. The synthetic process of the MnO_2/MCNT nano composite is described as follows. 0.1 g CNTs was weighed accurately and dispersed in 100 ml deionized [DI] water by ultrasonic vibration about 2 h. Subsequently, 0.665 g commercial sample of MnO_2 added with 15 ml of HCl and 15 ml DI water and it was added slowly into the above suspension. Then mixed solution was stirred by a magnetic bar for 1 h. 15 ml of ammonia solution was added in drops till precipitate formed. Finally, the precipitate was filtered washed thoroughly with water and dried in an oven at 80 °C for 1 h. After drying the obtained sample was calcinated at 400 and 500 °C for 2 h.

3. CHARACTERIZATION

The XRD of nanocomposites was recorded with PANalytical X"Pert PRO X-ray diffractometer operated at 40 kV,30 mA using Cu K_α radiation with a wavelength of 1.5406 Å. The surface morphologies of acid-treated CNTs, MnO_2 powder, and the uncorporated MnO_2/MCNT nanocomposites were obtained from Field emission scanning electron microscopy (FESEM) using FEI - QUANTA–FEG 250.The Surface morphological studies of the MnO_2/CNT nanocomposites were further investigated by Transmission Electron Microscopy (TEM) by PHILIPS CM 200 OPERATED AT 20-200 Kv with resolution 2.4 Ao. The Composition of the synthesized sample was obtained from energy-dispersive X-ray (EDX) spectroscopy. The Optical properties of the prepared samples were done by Uv-visible spectrometer (Thermofisher –Helious alpha)., Fourier transform infrared (FTIR) spectra were recorded using (Thermofisher-Nickelo380) in the 4000–400 cm^{-1} range. Raman Spectra were recorded for MnO_2/MCNT nanocomposites with a Horiba Jobin Yvon high-resolution micro-Raman spectrometer, model HR 800.

4. RESULTS

4.1 XRD Studies

XRD patterns of the Preheated CNTs, MnO_2 powder, and the MnO_2/MCNT nanocomposites are shown in Figure 1.The XRD pattern of the CNTs shows diffraction peaks at 26.5° and 43.2° and these peaks are due to the (002) and (100) reflections of graphite, respectively. The diffraction peaks at 2θ = 28.8°, 37.5°, 56.2° and 60.3° correspond to (211),(301), (600) and (521) planes respectively. The XRD results were in good agreement with JCPDS standard data card no.44-014. The lattice parameters observed for MnO_2 are a = 9.7875 and c = 2.8600, which match with the standard values (JCPDS card PDF file no. 44-0141a = 9.7847, c = 2.863). The cell volume of caddice-clew-likeMnO_2 is 273.97 Å and this value is in agreement with the standard values (274.1 Å). The average grain size of the prepared MnO_2 crystal is calculated to be 32 nm according to the Scherrer equation $D = K\lambda/\beta\cos\theta$ using the strongest diffraction peak of (211) where D is crystal grain size (nm), K is the Scherrer constant (0.89), λ is the X-ray wavelength (0.154056 nm) for Cu K_α, β is the full width at half maximum (FWHM) of the peak (211), and θ is the angle of diffraction peak. The XRD pattern of the MnO_2 loaded CNT nanocomposite shows that the diffraction pattern of the birnessite-type MnO_2 phase could be observed. While the diffraction patterns of the CNTs is not seen in the figure due to the uniform coating of the MnO_2 layer. The XRD pattern of MnO_2/MCNT samples annealed at 400 and 500 °C confirms that the while increasing the annealing temperature the crystallinity of MnO_2 also increases.

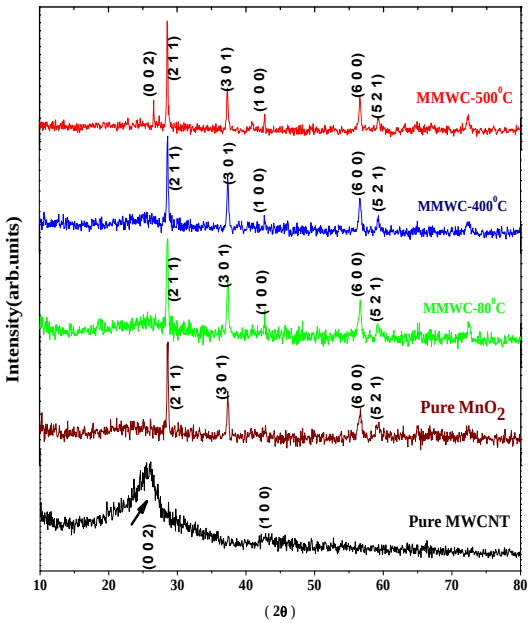

Fig.1: XRD patterns of (a) pristine CNTs, (b) pure MnO_2,and (c) MnO_2/MCNT nanocomposite.

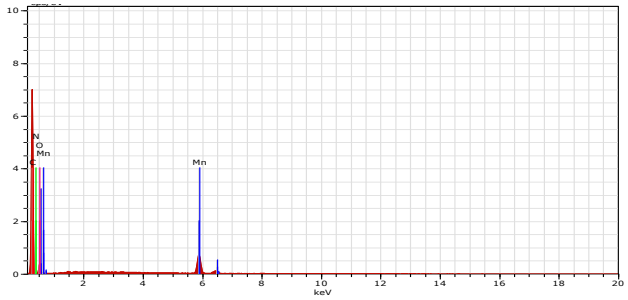

Fig.2: EDS spectrum of the MnO_2/MCNT nanocomposite.

One Day International Seminar on Materials Science & Technology (ISMST 2017)
4th August 2017
Organized by
Department of Physics, Mother Teresa Women's University, Kodaikanal, Tamilnadu, India

Energy dispersive spectrum of MnO_2 doped MCNT is shown in the figure 2. The EDS spectrum proved that the prepared sample shows the presence of Mn and O. When the annealing temperature was increased to 500 °C the amount of carbon content decreases while amount of MnO_2 content was increased. This shows at low annealing temperature the material is amorphous where as at high temperature it is crystalline in nature.

4.2 Optical Studies

In semi-conducting materials, the optical band energy gap (E_g) is obtained between the conduction and valence band. The band gap energy is obtained from Tauc relation.

$$\alpha h\gamma = A\,(h\gamma - E_g)^m$$

Where A is absorption coefficient given by $\alpha = 2.303 \log (T/d)$ (d is the thickness of the sample and T is the transmission coefficient), $h\gamma$ is the photon energy. Fig. 3 shows the plots of $(\alpha h\gamma)^2$ versus $h\gamma$ for all the samples under investigation. The values of E_g have been estimated by taking the intercept of the extrapolation to zero absorption with photon energy axis i.e. $(\alpha h\gamma)^2 = 0$.

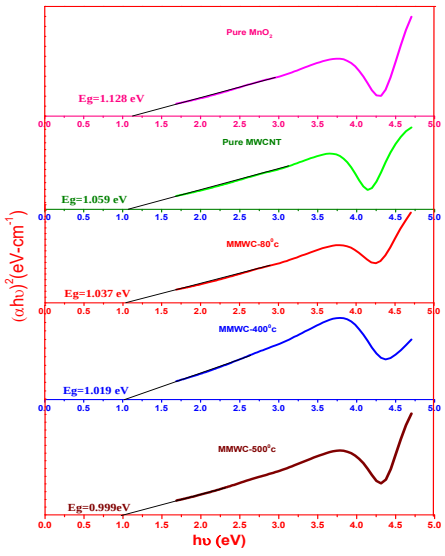

Fig.3: Tauc plot of the MnO_2, MCNT, MnO_2/MCNT nanocomposite at room temperature and annealed at 400 and 500 °C.

For MnO_2, Band gap value is obtained at 1.128 eV and this value decreases by the addition of MCNT to 1.037 eV in MnO_2 doped MCNT. Further the value of band gap was still reduced to 0.999 eV due to the annealing effect. Variation in the energy gap with annealing temperature and crystalline sizes was shown in the figure 4. As the crystalline size increases the band gap value started to decrease. The similar results were obtained with variation of bandgap and the annealing temperature. This decrease in bandgap value is due to several factors like grain size, carrier concentration, lattice strain etc. However in this study this decreasing trend is due to the decrease in grain size.

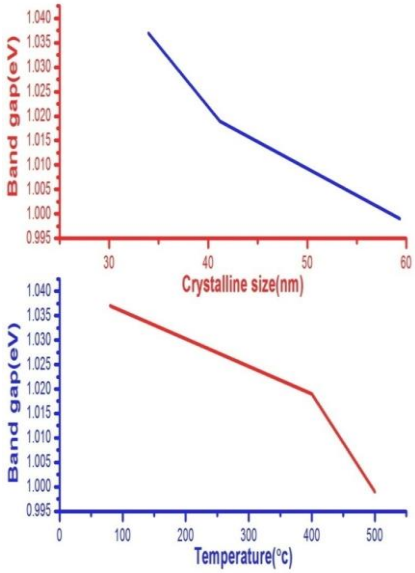

Fig.4: Variation of a) Bandgap with crystalline size and b) Bandgap with Annealing Temperature.

4.3 FTIR Studies

The FTIR spectra of as-prepared manganese dioxide (Fig.5) exhibited a very broad peak centered at 3400 cm^{-1} associated with the stretching vibration of OH groups of adsorbed water molecules. The bands at 1623 and 1415 cm^{-1} represented vibrations related to interactions of Mn with OH and other surface groups. A broad peak below 750 cm^{-1} is attributed to the vibrations of the Mn-O bonds. The peaks at 2920 and 2854 cm^{-1} correspond to the C–H stretch vibrations, originated from the surface of tubes. The intensities of peak obtained decreases with increase in annealing temperature, which suggests that the surface of MCNT has been covered by MnO_2.

One Day International Seminar on Materials Science & Technology (ISMST 2017)
4th August 2017
Organized by
Department of Physics, Mother Teresa Women's University, Kodaikanal, Tamilnadu, India

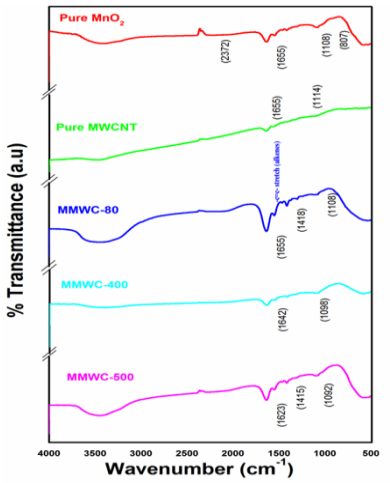

Fig.5: FTIR spectra of MCNT, MnO_2 and heat treated MnO_2 doped MCNT.

4.4 Raman Studies

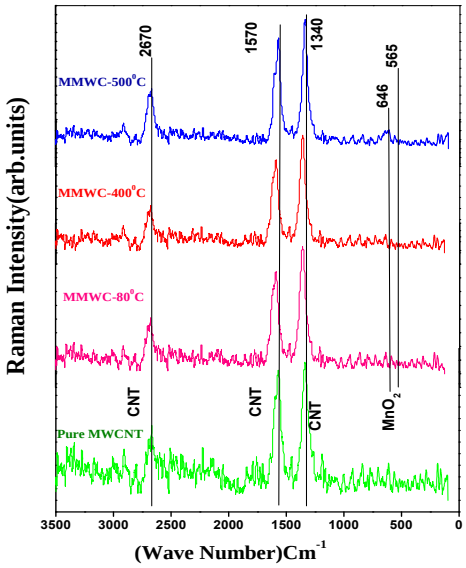

Fig. 6 Raman spectra of the pristine MCNT, as Prepared MnO_2/MCNT, MnO_2/MCNT at 400°C and 500°C

The Raman spectra of MnO_2 coated MCNT were shown in Fig.6. The three strongest Raman peaks at1570 (G band), 1340 (D band), and 2670 cm^{-1} (2D band) were assigned to pristine CNTs, which originate from the Raman-active, in-plane atomic displacement E_{2g} mode, disorder-induced features of the CNTs and the overtone of D band. The two weakest Raman bands at 565, and 646 cm^{-1}were confirmed the presence of MnO_2 with low quantity. Also it confirms the appeared peaks at 500 to 510, 575 to 585, and 625 to 650 cm^{-1}were due to two major vibrational features of the birnessite-type MnO_2 compounds and in good agreement with reported values. The Raman spectra result confirms the XRD results. The Synthesized samples are birnessite MnO_2 coated on MCNT.

4.4. Morphological Studies

The FESEM and TEM images of the birnessite-type MnO_2 powder, and the MnO_2/MCNT nanocomposite are shown in Figure 7. It can be observed in Figure 7A that the diameter of the CNTs is about 20 to 50 nm. When the annealing temperature was 400 °C the prepared MnO_2 doped MWCNT shows low number MnO_2 was attached with the MWCNT. While increasing the annealing temperature to 500 °C the MnO_2 particles decorated on the MWCNT (Fig.7C &D).

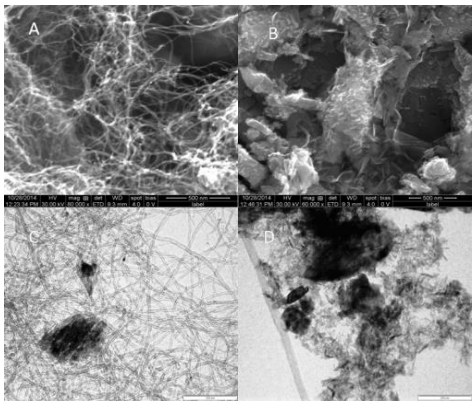

Fig.7: SEM images of Pure MCNT (A & B) and TEM images of MnO_2/MCNT nanocomposite annealed at 400 °C (C) & 500 °C (D).

5. CONCLUSION

MnO_2 incorporated MCNT were synthesized by a solvo thermal method. The synthesized samples were annealed at three different temperatures to improve the crystallinity of the sample. FESEM and TEM confirms the interconnection of MnO_2 over MCNT surface. EDS confirms the presence of Mn and O. The XRD patterns confirms the presence of MnO_2/MCNT by showing characteristic peaks and it also reveals that birnessite-type MnO_2.The crystallite size was obtained as 30nm calculated from scherrer formula. The bandgap value decrease from 1.037 to 0.999 eV reveals that the band gap shrinkage associated with Mn concentration more at high temperature phase. Raman studies confirmed that the appeared peaks at500 to 510, 575 to 585, and 625 to 650 cm^{-1}were due to two major vibrational features of the birnessite-type MnO_2 compounds. Due to highly porous structure and its high specific surface area of MnO_2/MCNT can be used as electrode material for electrochemical supercapacitors.

REFERENCES

[1] Liu .J, Xia .H, Xue .D.F, and Lu .L, Double-shelled nanocapsules of V_2O_5-based composites as high-performance anode and cathode materials for Li ion batteries, J. Am. Chem. Soc.131 (2009), pp. 12086–12087.

[2] Liu .D.Y and Reynolds .J.R.Dioxythiophene-based polymer electrodes for supercapacitor modules. Acs Appl Mater Interfaces. 2 (2010), pp. 3586–3593.

[3] Yu AP, Roes I, Davies A, et al. Ultrathin, transparent, and flexible graphene films for supercapacitor application. Appl Phys Lett. 96 (2010), pp. 253105.1–253105.3.

[4] Simon .P and Gogotsi .Y, Materials for electrochemical capacitors, Nat. Mater. 7 (2008),pp. 845–864.

[5] Yun DJ and Rhee SW. Composite Films of oxidized multiwall carbon nanotube and poly(3,4-ethylenedioxythiophene):polystyrene sulfonate (PEDOT: PSS) as a contact electrode for transistor and inverter devices. Acs Appl Mater Interfaces

[6] Hsu CL, Lin CTe, Huang JH, et al. Layer-by-layer graphene/TCNQ stacked films as conducting anodes for organic solarcells. Acs Nano. 6 (2012) pp. 5031–5039.

[7] Jun J, Lee JS, Shin DH, et al. Aptamer-functionalized hybrid carbon nanofiber FET-type electrode for a highly sensitive and selective platelet-derived growth factor biosensor. Acs Appl Mater Interfaces, 6 (2014), pp. 13859–13865.

[8] Qu .Q.T, Zhang .P, Wang .B, Chen .Y.H, Tian .S, Wu .Y.P, and Holze .R, Electrochemical performance of MnO2 nanorods in neutral aqueous electrolytes as a cathode for asymmetric supercapacitors, J. Phys. Chem. C 113 (2009), pp. 14020–14027.

[9] Wu.Z.S, Ren.W.C, Wang.D.W, Li.F, Liu.B.L, and Cheng.H.M, High-energy MnO_2 nanowire/graphene and graphene asymmetric electrochemical capacitors, ACS Nano 4 (2010), pp. 5835–5842.

[10] Li.L, Raji A.R, Fei H, et al. Nanocomposite of polyaniline nanorods grown on graphene nanoribbons for highly capacitive pseudocapacitors. Acs Appl Mater Interfaces. 5, (2013) pp.6622–6627.

[11] Xie.X.F and Gao.L, Characterization of a manganese dioxide/carbon nanotube composite fabricated using an in situ coating method, Carbon 45, (2007), pp. 2365–2373.

[12] Jiang H, Li CZ, Sun T, et al. High-performance supercapacitor material based on $Ni(OH)_2$ nanowire-MnO_2 nanoflakes coreshell nanostructures. Chem Commun 48, (2012), pp. 2606–2608.

[13] Hou Y, Cheng YW, Hobson T, Liu J. Design and synthesis of hierarchical MnO_2 nanospheres/carbon nanotubes /conducting polymer ternary composite for high performance electrochemical electrodes. Nano Lett. 10 (2010), pp. 2727–27233.

[14] Xia H, Lai MO, Lu L. Nanoflaky MnO2/carbon nanotube nanocomposites as anode materials for lithium-ion batteries.J Mater Chem 20(33):(2010) pp.6896–902.

[15] Xia H, Lai.M.O, and Lu.L, Nanostructured manganese oxide thin films as electrode material for supercapacitors, J. Miner. Met. Mater. Soc. 63 (2011), pp. 54–59.

[16] Gao.P.C, Lu.A.H, and Li.W.C, Dual functions of activated carbon in a positive electrode forMnO2-based hybrid supercapacitor, J. Power Sourc. 196 (2011), pp. 4095–4101.

[17] Yu AP, Roes I, Davies A, et al. Ultrathin, transparent, andflexible graphene films for supercapacitor application. Appl Phys Lett 96 (2010)pp. 253105.1–253105.3.

[18] Li YF, Liu YZ, Yang YG, et al. Reduced graphene oxide/MWCNT hybrid sandwiched film by self-assembly for high performance supercapacitor electrodes. Appl Phys A-Mater, 108 (2012) pp. 701–707.